Bone Reports 2 (2015) 36–43

Contents lists available at ScienceDirect

Bone Reports

journal homepage: www.elsevier.com/locate/bonr

Original Full Length Article

Mineral trioxide aggregate induces osteoblastogenesis via Atf6

Toyonobu Maeda [a], Atsuko Suzuki [a], Satoshi Yuzawa [a], Yuh Baba [b], Yuichi Kimura [c], Yasumasa Kato [a,*]

[a] Department of Oral Function and Molecular Biology, Ohu University School of Dentistry, Koriyama 963-8611, Japan
[b] Department of General Clinical Medicine, Ohu University School of Dentistry, Koriyama 963-8611, Japan
[c] Division of Endodontics, Department of Conservative Dentistry, Ohu University School of Dentistry, Koriyama 963-8611, Japan

ARTICLE INFO

Article history:
Received 12 February 2015
Accepted 26 March 2015
Available online 9 April 2015

Edited by Peter Ebeling

Keywords:
Osteoblastgenesis
Endodontics
Bone regeneration
Mineral trioxide aggregate
Atf6

ABSTRACT

Mineral trioxide aggregate (MTA) has been recommended for various uses in endodontics. To understand the effects of MTA on alveolar bone, we examined whether MTA induces osteoblastic differentiation using MC3T3-E1 cells. MTA enhanced mineralization concomitant with alkaline phosphatase activity in a dose- and time-dependent manner. MTA increased production of collagens (Type I and Type III) and matrix metalloproteinases (MMP-9 and MMP-13), suggesting that MTA affects bone matrix remodeling. MTA also induced *Bglap* (osteocalcin) but not *Bmp2* (bone morphogenetic protein-2) mRNA expression. We observed induction of *Atf6* (activating transcription factor 6, an endoplasmic reticulum (ER) stress response transcription factor) mRNA expression and activation of Atf6 by MTA treatment. Forced expression of p50Atf6 (active form of Atf6) markedly enhanced *Bglap* mRNA expression. Chromatin immunoprecipitation assay was performed to investigate the increase in p50Atf6 binding to the *Bglap* promoter region by MTA treatment. Furthermore, knockdown of Atf6 gene expression by introduction of Tet-on Atf6 shRNA expression vector abrogated MTA-induced mineralization. These results suggest that MTA induces in vitro osteoblastogenesis through the Atf6–osteocalcin axis as ER stress signaling. Therefore, MTA in endodontic treatment may affect alveolar bone healing in the resorbed region caused by pulpal infection.

1. Introduction

Mineral trioxide aggregate (MTA), which is a bioactive inorganic compound consisting of calcium silicate, calcium aluminate, calcium aluminoferrite, calcium sulfate, and bismuth oxide, has been clinically used for not only retrograde filling and apexification but also repair of accidental root perforations (Parirokh and Torabinejad, 2010; Bernabé et al., 2013). Several studies have postulated microleakage of MTA from the root in endodontic treatment (Lawley et al., 2004; Yazdizadeh et al., 2013) and the other reported induction and/or acceleration of bone repair of MTA in vivo (Qin et al., 2010; Wu et al., 2013). These findings conducted us to explore molecular mechanism(s) of healing action of MTA for the resorbed alveolar bone due to endodontic infection.

Osteoblasts differentiate into bone forming phenotype from mesenchymal stem cell precursors in response to several factors, such as bone morphogenetic proteins (BMPs), transforming growth factor (TGF) β1, and vascular endothelial growth factor (VEGF) (Maeda et al., 2003). Bone extracellular matrices (ECMs) consisting of Type I collagen, osteocalcin, bone sialoprotein, osteopontin, and decorin have critical roles in differentiation and mineralization. Generally, osteoblastogenesis is divided into three stages depending on differentiation using marker protein expression: e.g., alkaline phosphatase (ALP, early phase), bone sialoprotein (BSP, middle phase), osteopontin (middle phase), and osteocalcin (late phase). Osteocalcin is a vitamin K-dependent calcium-binding protein containing two or three γ-carboxyglutamic acid residues in the molecule (Maeda et al., 2004; Price and Baukol, 1980), and is abundant in the bone and teeth as a noncollagenous protein except dental enamel. *Bglap* gene knockout mice develop hyperostosis (Ducy et al., 1996).

The endoplasmic reticulum (ER) plays an important role in protein maturation through the folding process. Accumulation of unfolded proteins in the lumen of the ER disrupts ER homeostasis, which is known as "ER stress". The unfolded protein response (UPR) is an adaptive response to ER stress, and is widely conserved in eukaryotes for regulation of protein maturation and protection from cell death. The ER stress reaction element (ERSE) is *cis*-acting element with the consensus sequence CCAATN9CCACG, which is known to be recognized by NF-Y/CBF (Roy et al., 1996). Haze et al. (2001) also reported that the basic leucine zipper (bZIP) protein Atf6 (p50Atf6) binds to the CCAAT consensus sequence of ERSE. Atf6 is synthesized as a transmembrane precursor protein (p90Atf6) of 90 kDa in the ER. It translocates to the Golgi by

* Corresponding author at: Department of Oral Function and Molecular Biology, Ohu University School of Dentistry, 31-1 Misumido, Tomitamachi, Koriyama 963-8611, Japan.
E-mail addresses: t-maeda@den.ohu-u.ac.jp (T. Maeda), bebas963@yahoo.co.jp (A. Suzuki), s-yuzawa@den.ohu-u.ac.jp (S. Yuzawa), y-baba@den.ohu-u.ac.jp (Y. Baba), y-kimura@den.ohu-u.ac.jp (Y. Kimura), yasumasa-kato@umin.ac.jp (Y. Kato).

http://dx.doi.org/10.1016/j.bonr.2015.03.003

the ER chaperone BiP/GRP78 in response to ER stress and is cleaved by Ca^{2+}-dependent Golgi-associated proteinases (S1P and S2P) to release the transcriptionally active N-terminal fragment (p50Atf6) of 50 kDa including the bZIP sequence (Ye et al., 2000; Chen et al., 2002). Atf6 is thought to be a master regulator of the UPR to reduce ER stress along with two other molecules, i.e., IRE1 (inositol requiring 1) and PERK [PKR (protein kinase R)-like ER kinase] (Kaufman, 1999; Mori, 2000). Involvement ER stress signaling in osteoblastenesis has been reported (Jang et al., 2012; Liu et al., 2012; Wang et al., 2014a). In addition, Hino et al. (2010) showed that ER stress marker expression was down-regulated in osteoblasts of osteoporosis patients, suggesting ER stress play an important role for osteoblastic differentiation. Expansion of the ER capacity to prevent ER overload-induced apoptosis by increasing production of ECM proteins, such as Type I collagen (Tohmonda et al., 2011).

Although previous studies showed that MTA affected the differentiation of odontoblasts and bone marrow stromal cells with elevated expression of some genes, such as *Alp* (alkaline phosphatase), *Osx* (Sp7, osterix), *Bglap* (osteocalcin), and *Col1a1* (Type I collagen) (Min et al., 2008, 2009; Wang et al., 2014b; Zhao et al., 2012), molecular mechanism of MTA-induced bone healing mechanisms remains unclear. The present study was performed to determine whether MTA induces osteoblastic differentiation and tissue mineralization through the ER stress signaling pathway.

2. Materials & methods

2.1. Reagents

ProROOT MTA was provided by Dentsply (Johnson City, TN). Isogen total RNA extraction kit was purchased from Nippon Gene (Tokyo, Japan). SYBR Premix Ex Taq II and enzyme-linked immunosorbent assay (ELISA) kits for Mouse Gla-Osteocalcin and BMP-2 were from Takara (Tokyo, Japan) and R&D Systems (Minneapolis, MN), respectively. Alpha modified Eagle's MEM (αMEM) was from ICN Pharmaceuticals (Aurora, OH). Alkaline phosphatase (ALP) determination kit (Lab Assay ALP) were from Wako (Osaka, Japan). Blocking regent N102 was from NOF (Tokyo, Japan). Immobilon-P PVDF membranes and chemiluminescence reagent were from Merck Millipore (Billerica, MA). Avidin-conjugated horseradish peroxidase (HRP) was from Bio-Rad (Hercules, CA). Xfect Transfection Reagent was from Clontech (Mountain View, CA). Geneticin was from Roche (Basel, Switzerland). Doxycycline was from Sigma Aldrich (St-Louis, MO).

2.2. Vectors and transfection

The coding region of p50Atf6 was cloned by RT-PCR and inserted into the p3 × FLAG-CMV-10 vector (Sigma-Aldrich, St-Louis, MO) to intracellularly express N-terminal Flag-tagged p50Atf6 fusion protein. The shRNA for *Atf6* mRNA expression vector was constructed using the pSingle-tTS-shRNA vector (Clontech, Mountain View, CA) with an oligonucleotide targeting *Atf6*. Target sequence to construct an inducible shRNA expression vector for *Atf6* using the pSingle-tTS-shRNA vector was as follows: 5′-TCG AG***G CTC AGA CAT GAA GGC AGA*** TTC AAG AGA ***TCT GCC TTC ATG TCT GAG C***TT TTT TAC GCG T-3′, where the target in indicated in bold underlined italic font. The resultant plasmid was designated as pSingle-tTS-Atf6-shRNA. Vectors were transfected with Xfect Transfection Reagent (Clontech).

2.3. Antibodies

Rabbit polyclonal antibodies against Atf6 and Type I collagen were purchased from Abcam (Cambridge, UK). Rabbit polyclonal antibodies against Type III collagen were from Santa Cruz (Dallas, TX). Biotin-conjugated goat anti-rabbit IgG (H + L) was from Jackson ImmunoResearch (West Grove, PA). Anti-glyceraldehyde 3-phosphate dehydrogenase (GAPDH) antibody was from Gene Tex Inc. (Irvine, CA).

2.4. Cell and cell culture

MC3T3-E1 cells (a clonal pre-osteoblastic cell line derived from newborn mouse calvaria) were grown in growth medium consisting of αMEM supplemented with 10% fetal bovine serum (FBS) as described previously (Maeda et al., 2003). For differentiation of the cells, we used differentiation medium consisting of growth medium supplemented with 50 μg/mL ascorbate 2-phosphate, 10 mM β-glycerophosphate, and 40 mM HEPES (pH 7.4).

2.5. Preparation of MTA solution

The culture medium soluble fraction of MTA was used for this assay according to Hakki et al. (2009) with some modifications. MTA powder (1 g) was suspended in 50 mL of αMEM, swelled, and incubated for 2 weeks at 4 °C with gentle shaking to release biologically active substances from the powder. After centrifugation at 3000 × *g* for 15 min at 4 °C, the supernatant used as stock solution (20 mg-powder/mL) was diluted 20,000- and 8000-fold with αMEM to final concentrations of 1.0 μg/mL and 2.5 μg/mL, respectively, and used for the experiment as MTA solution. The IC_{50} was 9.5 μg/mL. MTA saturated solution at 2.5 μg/mL contained 2.3 μM calcium and showed negligible levels of mineral deposition without cells. It also did not affect the pH of the culture medium.

2.6. Alizarin Red S (AR-S) staining

Mineralized matrix in the plates was stained with AR-S. Briefly, cells were fixed in 70% ethanol for 1 h at room temperature, washed with Ca^{2+}- and Mg^{2+}-free Dulbecco's phosphate-buffered saline (PBS (−)), and stained with 40 mM AR-S at pH 4.2 for 10 min at room temperature. Next, they were washed five times with deionized water and incubated in PBS (−) for 15 min to eliminate nonspecific staining. The stained matrix was photographed using a digital camera. The red stain was quantified using Molecular Imager (BioRad, Hercules, CA).

2.7. Measurement of ALP activity

The membrane fraction of the cells was extracted with 0.1 M Tris–HCl (pH 7.2) containing 0.1% Triton X-100. ALP activity was determined using a Lab Assay ALP kit (Wako, Osaka, Japan).

2.8. Measurement of osteocalcin and BMP-2 in conditioned medium (CM)

Each time point, culture medium was replaced with fresh medium without FBS and cells were cultured for a further 24 h. CM from 24-hour cultures were collected and concentrated by acetone precipitation. Osteocalcin and BMP-2 were measured by enzyme-linked immunosorbent assay (ELISA).

2.9. Inducible knockdown system

For knockdown of the mouse *Atf6* gene, we used the Knockout Single Vector Inducible RNAi System. The sequence targeting *Atf6* was cloned into the pSingle-tTS-shRNA vector. Stably transfected cells were selected by geneticin. Cloned cells showed significant reduction of *Atf6* mRNA product in the presence of 1 μg/mL doxycycline (Dox).

2.10. Real-time reverse-transcription polymerase chain reaction (RT-PCR)

Total RNA was isolated with Isogen, and reverse-transcribed to synthesize cDNA with a High-Capacity cDNA Reverse Transcription Kit (Life Technologies, Rockville, MD). Resultant cDNA samples were amplified

by SYBR Premix Ex *Taq* II with specific primers in a Thermal Cycler Dice Real Time System (TP-870; Takara, Tokyo, Japan). The level of *Actb* (β-actin) mRNA was used as an internal control. The specific primer sequences used are shown in Table 1.

2.11. Western blotting

Western blotting was performed essentially as described in our previous reports (Kato et al., 2005). Whole-cell lysates (10 μg/lane) were separated by 7.5% or 10% SDS-polyacrylamide gel electrophoresis (SDS-PAGE) and transferred onto Immobilon-P PVDF membranes. Membranes were blocked with TBS-T (20 mM Tris–HCl, pH 7.5, 150 mM NaCl, and 0.05% Tween 20) containing 20% blocking regent N102, treated with first antibody followed by incubation with biotin-conjugated secondary antibody and avidin-conjugated horseradish peroxidase. Signals were detected with enhanced chemiluminescence reagents. In some cases, antibodies were stripped off from the membrane with stripping buffer consisting of 6 M guanidine hydrochloride, 20 mM Tris–HCl (pH 7.5), 0.2% Nonidet P-40, and 0.1 M β-mercaptoethanol (Yeung and Stanley, 2009). Anti-GAPDH antibody was used as a loading control.

2.12. Gelatin and casein substrate zymography

Zymography was performed as described in our previous reports (Kato et al., 2005). Briefly, gelatinlytic and caseinolytic activity in CM were detected by 7.5% SDS-PAGE containing 0.1% gelatin or casein, respectively. SDS in the gel was removed by Triton X-100 and enzyme reaction was carried out in the presence of 10 mM $CaCl_2$. The destained bands in the gels, indicating proteolytic activities, were quantified using Molecular Imager (BioRad, Hercules, CA).

2.13. Chromatin immunoprecipitation (ChIP) assay

ChIP was performed as described previously (Agata et al., 2001). Briefly, MC3T3-E1 cells were fixed with 1% formaldehyde and sonicated. Target protein in the sample was precipitated by anti-Atf6 antibody or non-immune IgG as a control. Real-time PCR was performed with the co-precipitated oligonucleotide as the template. Input DNA was also amplified by PCR for normalization. Primer sequences for ChIP assay are shown in Table 1.

Table 1
Primer sequences.

Targets		Sequences	Product size (bp)
Atf6	Forward	GAT GCC TTG GGA GTC AGA CC	162
	Reverse	CCA ACT CCT CAG GAA CGT GCT	
Bglap	Forward	GTG AGC TTA ACC CTG CTT GT	96
	Reverse	AGC ACA GGT CCT AAA TAG TGA TAC C	
Bglap promoter	Forward	CAA TCA CCT ACC ACA GCA TCC TTT GGG T	77
	Reverse	GGG GAT GCT GCC AGG ACT AAT TGG G	
Bmp2	Forward	TGA CTG GAT CGT GGC ACC TC	112
	Reverse	CAG AGT CTG CAC TAT GGC ATG GTT A	
Bmp4	Forward	AGC CGA GCC AAC ACT GTG AG	68
	Reverse	TCA CTG GTC CCT GGG ATG TTC	
Col1a1	Forward	GAC ATG TTC AGC TTT GTG GAC CTC	119
	Reverse	GGG ACC CTT AGG CCA TTG TGT A	
Col3a1	Forward	AAC GGA GCT CCT GGC CCC AT	113
	Reverse	CCA TCA CTG CCC CGA GCA CC	
Mmp9	Forward	GCC CTG GAA CTC ACA CGA CA	85
	Reverse	TTG GAA ACT CAC ACG CCA GAA G	
Mmp13	Forward	TCC CTG GAA TTG GCA ACA AAG	120
	Reverse	GCA TGA CTC TCA CAA TGC GAT TAC	
Actb	Forward	CAT CCG TAA AGA CCT CTA TGC CAA C	171
	Reverse	ATG GAG CCA CCG ATC CAC A	

3. Results

3.1. Promotion of mineralization in MC3T3-E1 cells by MTA

First, we examined whether MTA affects mineralized nodule formation by osteoblastic MC3T3-E1 cells. Alizarin Red-S staining showed that MTA induced nodule formation in a dose-dependent manner (Fig. 1A and B). ALP activity was also induced dose-dependently by MTA, and statistical significance was confirmed from day 8 and later (Fig. 1C).

3.2. MTA increases collagen (Col1a1 and Col3a1) and MMP (Mmp9 and Mmp13) mRNA expression

Type I collagen is a major extracellular matrix protein in bone. On the other hand, Type III collagen, which is a fibril-forming collagen, is an important factor for formation of Type I collagen fibers. MTA induced accumulation of both Col1a1 and Col3a1 at mRNA expression level (Fig. 2A–E). It should be noted that the maximum induction of *Col3a1* mRNA expression (day 4) occurred earlier than that of *Col1a1* mRNA expression (day 8) (Fig. 2D and E). This was in good agreement with the roles of Type I and Type III collagen in fiber formation.

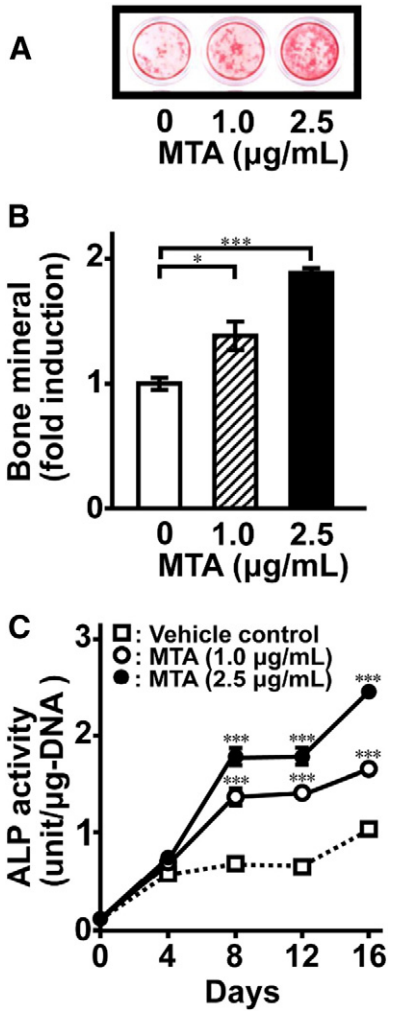

Fig. 1. MTA induces mineralization of extracellular matrix in MC3T3-E1 cells. The cells were cultured for 16 days in the absence or presence of MTA at indicated concentrations. (A) AR-S staining was performed to examine mineralized nodule formation. (B) A quantitative analysis of the intensity for AR-S staining was determined by Molecular Imager FX (Bio-Rad). (C) The time course of stimulation of ALP activity by MTA in MC3T3-E1 cells. ALP samples from whole-cell extracts were assayed using an ALP kit. Data represent the means ± SEM ($n = 4$). Statistical significance of differences between MTA treated group and corresponding time-matched vehicle control is indicated by $^{*}P < 0.05$ and $^{***}P < 0.001$.

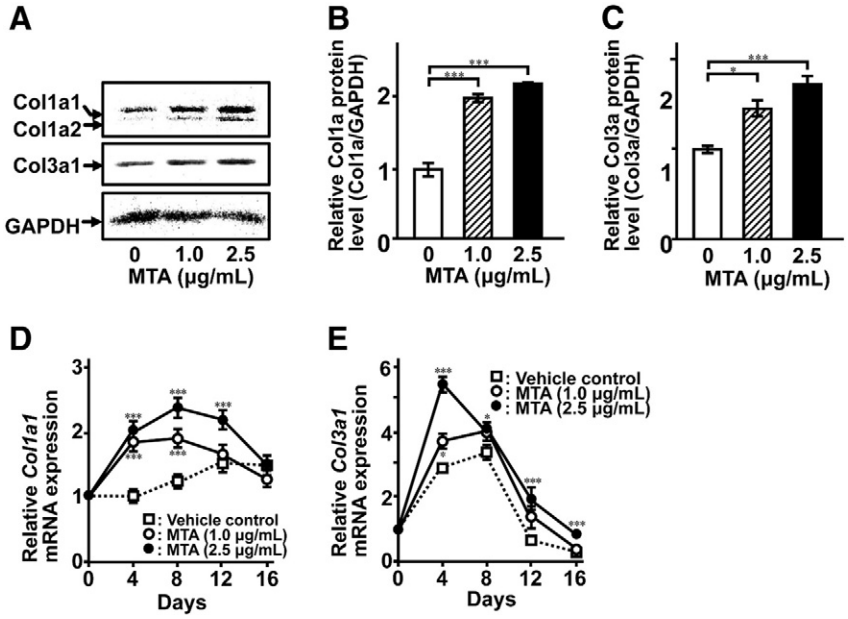

Fig. 2. MTA induces collagen synthesis in MC3T3-E1 cells. (A) The cells were cultured for 8 days in the absence or presence of MTA at indicated concentrations. Whole-cell lysates were subjected to western blotting (A). A quantitative analysis of intensity for each immunoreacted band for Type I collagen α1 (Co1a) (B) and Type III collagen α1 (Col3a) (C) was performed by Molecular Imager FX (Bio-Rad). Total RNA was extracted, reverse-transcribed and amplified by real-time PCR with primer sets for *Col1a1* and *Col3a1*. Data are expressed as mean ± SEM ($n = 4$). Statistical significance of differences between MTA treated group and corresponding time-matched vehicle control is indicated by $^{*}P < 0.05$ and $^{***}P < 0.001$.

MMP-13 cleaves Type I and Type III collagens at specific sites generating 3/4 N-terminal and 1/4 C-terminal fragments, as the major fibrous collagen-degrading proteinase in mice. These fragments are rapidly denatured at physiological temperature and are degraded by MMP-2 and MMP-9. MTA significantly induced production of MMP-9 and MMP-13 at both mRNA and protein level, while their active forms were negligible level (Fig. 3). Maximum mRNA levels of both molecules were observed on day 12 (Fig. 3C and F). This elevation was observed at a later phase compared to the collagen expression peaks (see Fig. 2D and E), and it showed good agreement with the osteocalcin expression peak (Fig. 4).

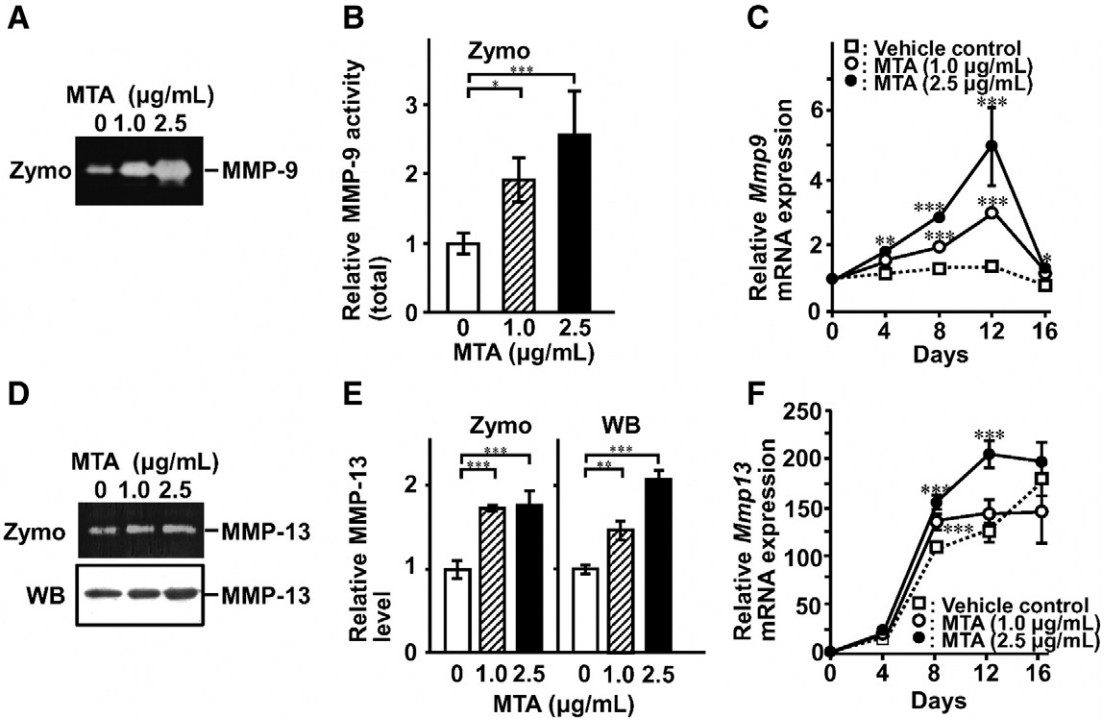

Fig. 3. Production of MMPs in MTA-treated MC3T3-E1 cells. The cells were cultured in the absence or presence of MTA for 12 days. The medium was changed to serum-free conditioned medium. After 24 h, the conditioned medium was collected and concentrated. (A) MMP-9 was detected by gelatin-zymography as the precursor. (D) MMP-13 was detected by casein-zymography and western blotting as the precursor. A quantitative analysis of the intensity of each band was performed by Molecular Imager FX (Bio-Rad) (B and E). Total RNA was extracted and determined mRNA expression of *Mmp9* (C) and *Mmp13* (F) by real-time RT-PCR. Data represent the means ± SEM ($n = 4$). Statistical significance of differences between MTA treated group and corresponding time-matched vehicle control is indicated by $^{*}P < 0.05$, $^{**}P < 0.01$ and $^{***}P < 0.001$. Zymo, zymography; WB, western blotting.

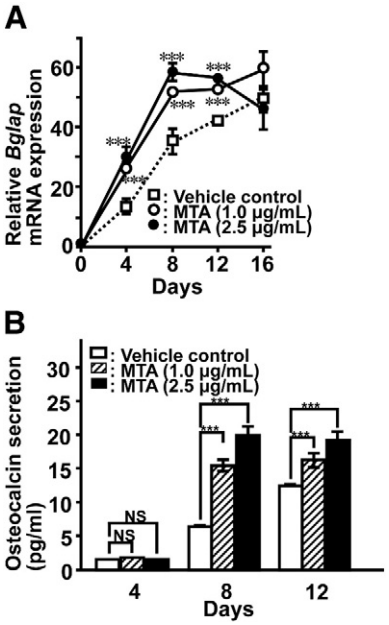

Fig. 4. Time course of *Bglap* mRNA expression (A) and osteocalcin secretion (B) in MTA-treated MC3T3-E1. At the indicated time points, total RNA was extracted for real-time RT-PCR. To determine osteocalcin secretion, culture medium was replaced with fresh medium and the cells were further cultured with or without MTA at the indicated concentration for 24 h. Osteocalcin concentration was measured using a mouse osteocalcin ELISA kit. Data represent the means ± SEM. Statistical significance of differences between MTA treated group and corresponding time-matched vehicle control is indicated by $^{***}P < 0.001$. NS, not significant.

3.3. Contribution of ER stress signaling to Bglap mRNA expression induced by MTA

As BMP signal through the expression of Runx2 enhances *Bglap* gene expression (Guo et al., 2012; Liu et al., 2013) and the *Bglap* gene was also driven by Atf6 (Jang et al., 2012), we examined Bmp-2, Bmp-4, and Atf6 expression in the presence or absence of MTA. MTA treatment affected neither BMP-2 nor BMP-4 expression (Fig. 5A–C). Similarly, there was no significant difference in BMP-2 protein level between MTA treated and untreated control groups.

Interestingly, *Atf6* gene expression was significantly upregulated by MTA treatment on day 8 as the maximum induction (Fig. 5D), while mRNA levels of the other ER stress signaling transducer such as Atf4 and OASIS (old astrocyte specifically induced substance) were not changed (data not shown). Western blotting analysis showed a significant increase in Atf6 production by MTA treatment (Fig. 5E). As the activation ratio (p50Atf6 vs. total Atf6; 0.54 in control, 0.47 in 1 μg/mL MTA, 0.45 in 2.5 μg/mL MTA) did not change markedly, it was suggested that the MTA-induced increase in p50Atf6, the active form of Atf6, was due to enhancement of production rather than its activation efficiency (Fig. 5F).

3.4. Atf6 contributes to MTA-stimulated mineralization

To obtain direct evidence regarding the contribution of Atf6 in MTA-stimulated bone formation, we investigated whether p50Atf6 was transcriptionally active by MTA treatment. Because p50Atf6 drives the *Bglap* gene promoter (Jang et al., 2012), we performed ChIP assay for the promoter region of *Bglap* gene. Expectedly, MTA treatment led to more significant binding Atf6 to the promoter region of the *Bglap* gene (Fig. 6).

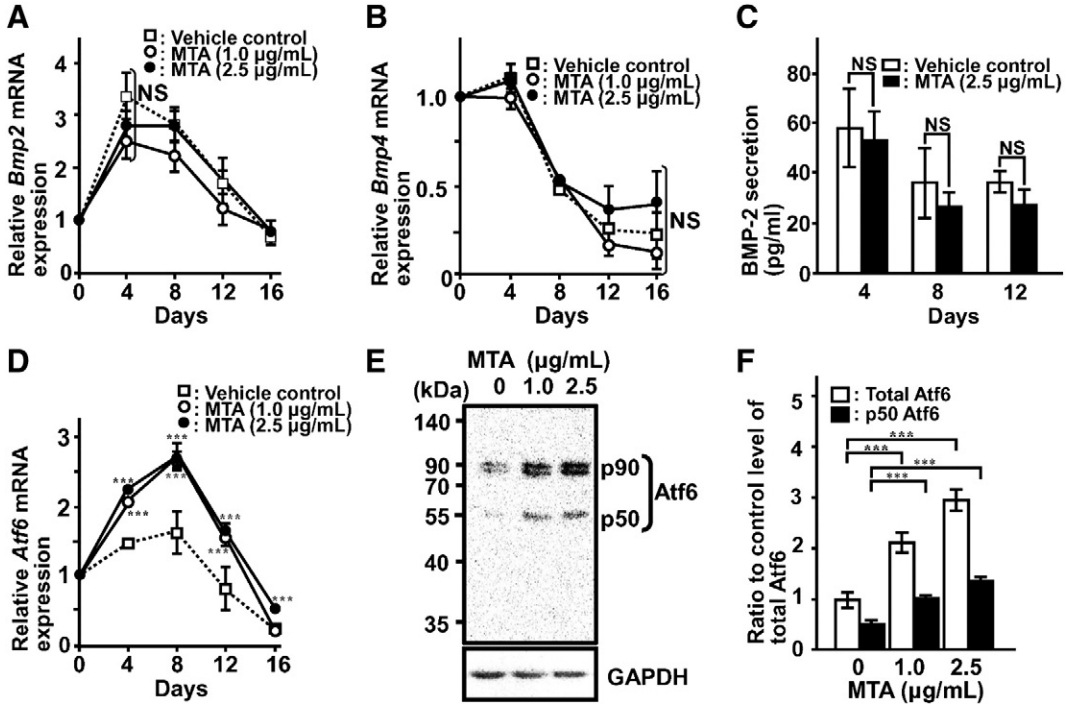

Fig. 5. MTA induced Atf6 expression but did not BMP-2 and 4 in MC3T3-E1 cells. Total RNA was extracted, reverse-transcribed, and amplified by real-time PCR using specific primer sets for *Bmp2* (A), *Bmp4* (B), and *Atf6* (D). (C) To determine BMP-2 protein secretion, culture medium was replaced with fresh medium at the indicated time points and the culture was continued with or without MTA for 24 h. The CM was analyzed for BMP-2 concentration using a BMP-2 ELISA Kit. (E) The cells were cultured for 12 days in the absence or presence of MTA at indicated concentration. Whole-cell lysates were subjected to immunoblotting with anti-Atf6 and GAPDH antibodies. (F) A quantitative analysis of the intensity of each band was performed by Molecular Imager FX (Bio-Rad). Total Atf6 was calculated as sum of intensities of p90 and p50 bands. Data represent the means ± SEM ($n = 3$). Statistical significance of differences between MTA treated group and corresponding time-matched vehicle control is indicated by $^{***}P < 0.001$. NS, not significant.

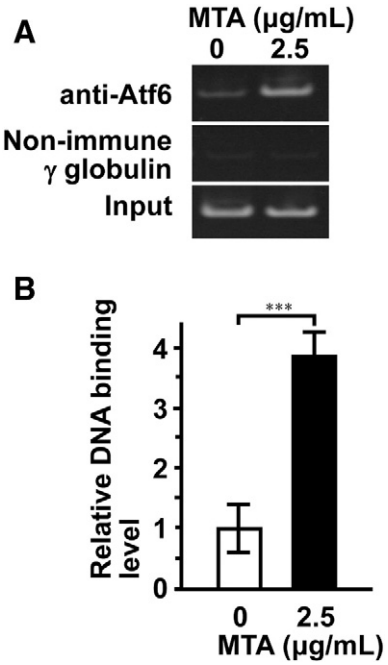

Fig. 6. MTA stimulates Atf6 binding to promoter region of *Bglap* gene. The cells were stimulated by MTA for 4 days. ChIP assays were performed. Cell lysates were incubated with non-immune IgG control or ATF6 antibodies. (A) PCR amplification of *Bglap* gene promoters was performed using immunoprecipitated and non-immunoprecipitated (input) DNA by using PCR thermal cycler. (B) A quantitative study of immunoprecipitated DNA was performed by using real-time PCR. Data represent the means ± SEM ($n = 3$). Statistical significance of differences between MTA treated group and corresponding time-matched vehicle control is indicated by $^{***}P < 0.001$.

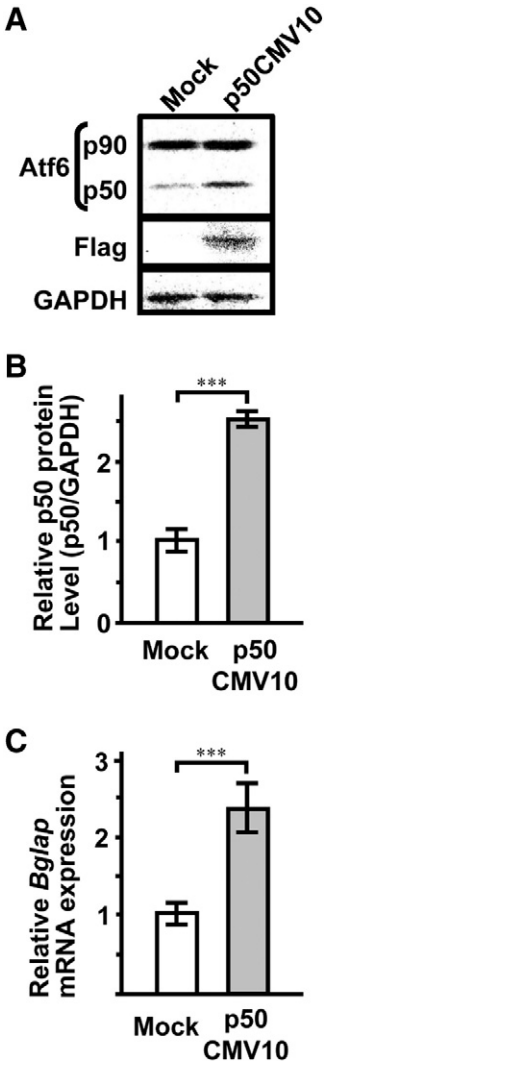

Fig. 7. Forced expression of active Atf6 (p50Atf6) induces *Bglap* gene expression. The cells were transiently transfected with a p3 × FLAGp50CMV10 or mock (p3 × FLAGCMV10) in MC3T3-E1 cells and cultured for 2 days in osteogenic medium. (A) Protein level of Atf6 was analyzed by western blotting. (B) A quantitative study of intensity was performed by Molecular Imager FX (Bio-Rad). (C) *Bglap* (osteocalcin) mRNA expression was determined by real-time RT-PCR. Data represent the means ± SEM ($n = 3$). ***, $P < 0.001$.

In addition, we constructed a Flag-tagged p50Atf6 (constitutively active Atf6) expression vector and investigated if forced expression of active Atf6 induces *Bglap* gene expression. Transient expression of the dominant active Atf6 protein, the level of which was 2.5-fold higher than the mock control, significantly upregulated *Bglap* mRNA expression (Fig. 7).

Finally, we investigated whether Atf6 contributes to MTA-stimulated mineralization. We constructed a Dox-inducible shRNA expression vector for Atf6 (pSingle-tTS-Atf6-shRNA) according to the Tet-on single-vector inducible RNA interference system. After transfection of pSingle-tTS-Atf6-shRNA vector into cells, stably transfected cells, which were selected by geneticin, were cloned and obtained for mineralization assay. Our data clearly showed that reduction of Atf6 expression by addition of Dox attenuated MTA-stimulated *Bglap* mRNA expression (Fig. 8) and also mineralization (Fig. 9) to a level equivalent to that of the control. These data suggested that MTA contributed to bone formation at least in part through Atf6.

4. Discussion

Osteoblast differentiation is regulated by a number of hormones and factors, such as TGF-β (transforming growth factor-β), BMP-2, and bFGF (basic fibroblast growth factor) (Hurley et al., 1994). Among them, BMP-2 is the most effective inducer of proliferation, differentiation, and mineralization in osteoblasts (Higuchi et al., 2002; Hiraki et al., 1991). Previous studies have shown that MTA promoted osteoblastic mineralization concomitant with increased BMP-2 mRNA expression (Ghasemi et al., 2014; Jeong et al., 2014). Here, we also investigated MTA-induced osteoblastic mineralization without BMP-2 mRNA elevation compared to controls. Several recent reports have revealed the contribution of ER stress signaling in osteoblastic differentiation. For example, Atf4 is enriched in osteoblasts and acts as a downstream effector of PERK (pancreatic ER kinase) through elf-2α activation in ER stress signaling to induce *Bglap* mRNA expression (Saito et al., 2011). In addition, it has been reported that Atf6 upregulates *Bglap* mRNA level (Jang et al., 2012) and that OASIS (old astrocyte specifically induced substance), which is a member of the CREB/Atf family, is highly expressed in osteoblasts and contributes to bone formation (Murakami et al., 2009). In the present study, we examined the expression of ER stress signaling transducers, such as Atf4, Atf6, and OASIS. Among them, only Atf6 expression was upregulated by MTA treatment. Moreover, p50 the activated form Atf6 was dose-dependently increased by addition of MTA. Because Atf6 plays an important role of differentiation in both odontoblast (Kim et al., 2014) and osteoblast (Jang et al., 2012), we examined whether Atf6 is the candidate "MTA activated transcription factor" to induce osteoblastic differentiation. As expected, MTA induced *Bglap* mRNA expression in a BMP-2-independent manner. Mineralized nodule formation was enhanced by MTA treatment, but its timing was not changed. Therefore, it was suggested that MTA induced osteoblastic differentiation at a rather late phase.

ER stress signaling plays an important role for expansion of the ER capacity to prevent ER overload-induced apoptosis by increasing production of ECM proteins, such as Type I collagen, and it is also associated with osteoblastic differentiation (Hino et al., 2010; Tohmonda et al., 2011). Here, we showed enhancement of tissue mineralization by

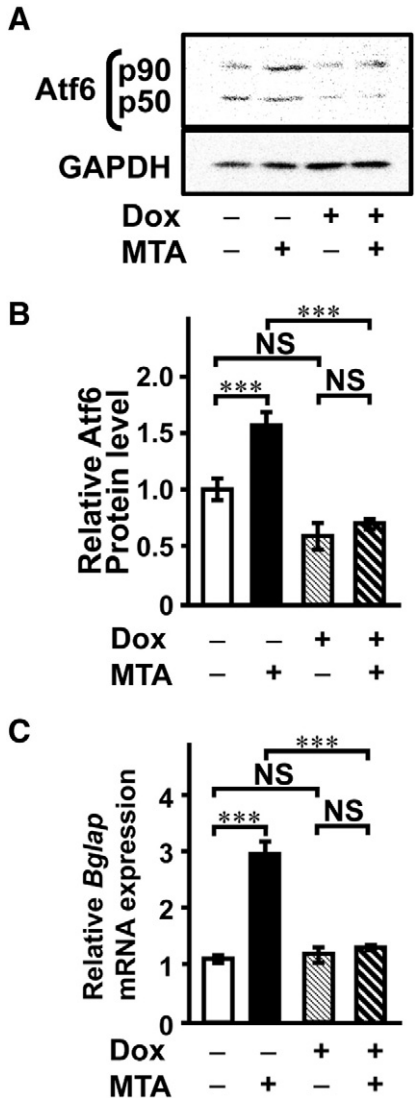

Fig. 8. Knockdown of *Atf6* gene expression abolishes *Bglap* mRNA expression and mineralization by MTA. Stable clones of *Atf6* shRNA were incubated with (+) or without (−) Dox and/or MTA for 16 days: MTA, 2.5 μg/mL; Dox, 1.0 μg/mL. (A) Whole-cell lysates were subjected to immunoblotting with anti-Atf6 and GAPDH antibodies on day 12 in culture. (B) A quantitative study for the intensity was performed by Molecular Imager FX (Bio-Rad). (C) *Bglap* mRNA expression was decreased by *Atf6* shRNA. On day 12 in culture, total RNA was extracted from the cells, reverse-transcribed, and subjected to qPCR analysis. Data represent the means ± SEM ($n = 3$). ***, $P < 0.001$; NS, not significant.

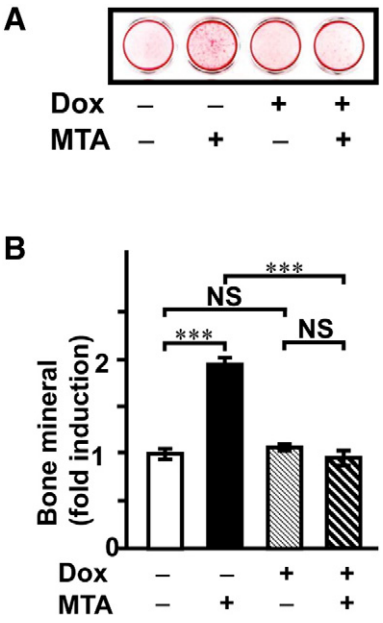

Fig. 9. Attenuation of Atf6 expression does not induce mineralized nodule formation in MTA-treated cells. The cells were cultured with (+) or without (−) Dox and/or MTA for 16 days: MTA, 2.5 μg/mL; Dox, 1.0 μg/mL. (A) AR-S staining was performed to examine mineralized nodule formation. (B) A quantitative study of the intensity of the AR-S staining was determined by Molecular Imager FX (Bio-Rad) (B, E). Data represent the means ± SEM ($n = 3$). ***, $P < 0.001$; NS, not significant.

MTA is probably due to not simple induction of collagen production but also activation of collagen remodeling. To accumulate and form collagen fibers, Type III collagen has been shown to trigger Type I collagen fibrillogenesis (Liu et al., 1997). In addition, Type III collagen has growth stimulatory activity for osteoblasts (Maehata et al., 2007). Our data indicated that MTA increased not only both Types I and III collagen synthesis but also MMP-9 and MMP-13 expression. Several studies have shown that induction of osteoblastic differentiation concomitantly increased MMPs. For example, osteoblastic differentiation induced by ascorbate 2-phosphate concomitantly enhanced both MMP-9 and MMP-13 production (Mizutani et al., 2001). The proteolytic cascade by MMP-2/MMP-13/MT1-MMP was shown to be involved in osteoblastic differentiation through mechanical forces (Barthelemi et al., 2012). In addition, osterix, a master regulator of osteoblastic differentiation, induced both MMP-1 (Nakashima et al., 2002) and MMP-13 (Zhang et al., 2012). Our data indicated that maximal induction of Types III and I collagen gene expression by MTA appeared on days 4 and 8, respectively. *Mmp-9* and *Mmp-13* mRNA expression were seen on day 12, just before mineralization. Taken together, it seemed reasonable that MTA induced MMPs during osteoblastic differentiation through collagen remodeling.

Our preliminary experiment showed strong toxicity for osteoblasts near to the MTA disk. Therefore, we used the medium-soluble fraction of MTA, according to the protocol (Hakki et al., 2009). The medium-soluble fraction, which may contain biologically active substances released from MTA, did not show any obvious toxicity for MC3T3-E1 cells, but stimulated MMP, collagen, and osteocalcin mRNA expression. Although MTA contains calcium silicate, bismuth oxide, and calcium aluminate (Camilleri, 2008), the ratio of substances released from MTA may differ according to the protocol. This may explain the discrepancies regarding BMP-2 expression by MTA. Our data, at least in part, suggested that substances released from MTA in the root were able to diffuse and affect distal osteoblasts in alveolar bone for late-stage differentiation and tissue mineralization in vivo through ER stress signaling.

5. Conclusions

Hashiguchi et al. (2011) investigated that MTA inhibits bone resorption. Taken together, we concluded that MTA in endodontic treatment may affect alveolar bone healing in the resorbed region caused by pulpal infection.

Conflict of interest

The authors confirm that there are no known conflicts of interest associated with this publication and there has been no significant financial support for this work that could have influenced its outcome.

Acknowledgments

A part of this work was supported by JSPS KAKENHI Grant (#21791862 and #10382756).

References

Agata, Y., Katakai, T., Ye, S.K., Sugai, M., Gonda, H., Honjo, T., et al., 2001. Histone acetylation determines the developmentally regulated accessibility for T cell receptor γ gene recombination. J. Exp. Med. 193, 873–880.

Barthelemi, S., Robinet, J., Garnotel, R., Antonicelli, F., Schittly, E., Hornebeck, W., et al., 2012. Mechanical forces-induced human osteoblasts differentiation involves MMP-2/MMP-13/MT1-MMP proteolytic cascade. J. Cell. Biochem. 113, 760–772.

Bernabé, P.F., Azuma, M.M., Ferreira, L.L., Dezan-Júnior, E., Gomes-Filho, J.E., Cintra, L.T., 2013. Root reconstructed with mineral trioxide aggregate and guided tissue regeneration in apical surgery: a 5-year follow-up. Braz. Dent. J. 24, 428–432.

Camilleri, J., 2008. The chemical composition of mineral trioxide aggregate. J. Conserv. Dent. 11, 141–143.

Chen, X., Shen, J., Prywes, R., 2002. The luminal domain of ATF6 senses endoplasmic reticulum (ER) stress and causes translocation of ATF6 from the ER to the Golgi. J. Biol. Chem. 277, 13045–13052.

Ducy, P., Desbois, C., Boyce, B., Pinero, G., Story, B., Dunstan, C., et al., 1996. Increased bone formation in osteocalcin-deficient mice. Nature 382, 448–452.

Ghasemi, N., Rahimi, S., Lotfi, M., Solaimanirad, J., Shahi, S., Shafaie, H., et al., 2014. Effect of mineral trioxide aggregate, calcium-enriched mixture cement and mineral trioxide aggregate with disodium hydrogen phosphate on BMP-2 production. Iran. Endod. J. 9, 220–224.

Guo, Y., Zhang, C.Q., Zeng, Q.C., Li, R.X., Liu, L., Hao, Q.X., et al., 2012. Mechanical strain promotes osteoblast ECM formation and improves its osteoinductive potential. Biomed. Eng. Online 11, 80.

Hakki, S.S., Bozkurt, S.B., Hakki, E.E., Belli, S., 2009. Effects of mineral trioxide aggregate on cell survival, gene expression associated with mineralized tissues, and biomineralization of cementoblasts. J. Endod. 35, 513–519.

Hashiguchi, D., Fukushima, H., Yasuda, H., Masuda, W., Tomikawa, M., Morikawa, K., et al., 2011. Mineral trioxide aggregate inhibits osteoclastic bone resorption. J. Dent. Res. 90, 912–917.

Haze, K., Okada, T., Yoshida, H., Yanagi, H., Yura, T., Negishi, M., et al., 2001. Identification of the G13 (cAMP-response-element-binding protein-related protein) gene product related to activating transcription factor 6 as a transcriptional activator of the mammalian unfolded protein response. Biochem. J. 355, 19–28.

Higuchi, C., Myoui, A., Hashimoto, N., Kuriyama, K., Yoshioka, K., Yoshikawa, H., et al., 2002. Continuous inhibition of MAPK signaling promotes the early osteoblastic differentiation and mineralization of the extracellular matrix. J. Bone Miner. Res. 17, 1785–1794.

Hino, S., Kondo, S., Yoshinaga, K., Saito, A., Murakami, T., Kanemoto, S., et al., 2010. Regulation of ER molecular chaperone prevents bone loss in a murine model for osteoporosis. J. Bone Miner. Metab. 28, 131–138.

Hiraki, Y., Inoue, H., Shigeno, C., Sanma, Y., Bentz, H., Rosen, D.M., et al., 1991. Bone morphogenetic proteins (BMP-2 and BMP-3) promote growth and expression of the differentiated phenotype of rabbit chondrocytes and osteoblastic MC3T3-E1 cells in vitro. J. Bone Miner. Res. 6, 1373–1385.

Hurley, M.M., Abreu, C., Gronowicz, G., Kawaguchi, H., Lorenzo, J., 1994. Expression and regulation of basic fibroblast growth factor mRNA levels in mouse osteoblastic MC3T3-E1 cells. J. Biol. Chem. 269, 9392–9396.

Jang, W.G., Kim, E.J., Kim, D.K., Ryoo, H.M., Lee, K.B., Kim, S.H., et al., 2012. BMP2 protein regulates osteocalcin expression via Runx2-mediated Atf6 gene transcription. J. Biol. Chem. 287, 905–915.

Jeong, Y., Yang, W., Ko, H., Kim, M., 2014. The effects of bone morphogenetic protein-2 and enamel matrix derivative on the bioactivity of mineral trioxide aggregate in MC3T3-E1cells. Restor. Dent. Endod. 39, 187–194.

Kato, Y., Lambert, C.A., Colige, A.C., Mineur, P., Noël, A., Frankenne, F., et al., 2005. Acidic extracellular pH induces matrix metalloproteinase-9 expression in mouse metastatic melanoma cells through the phospholipase D-mitogen-activated protein kinase signaling. J. Biol. Chem. 280, 10938–10944.

Kaufman, R.J., 1999. Stress signaling from the lumen of the endoplasmic reticulum: coordination of gene transcriptional and translational controls. Genes Dev. 13, 1211–1233.

Kim, J.W., Choi, H., Jeong, B.C., Oh, S.H., Hur, S.W., Lee, B.N., et al., 2014. Transcriptional factor ATF6 is involved in odontoblastic differentiation. J. Dent. Res. 93, 483–489.

Lawley, G.R., Schindler, W.G., Walker 3rd, W.A., Kolodrubetz, D., 2004. Evaluation of ultrasonically placed MTA and fracture resistance with intracanal composite resin in a model of apexification. J. Endod. 30, 167–172.

Liu, X., Wu, H., Byrne, M., Krane, S., Jaenisch, R., 1997. Type III collagen is crucial for collagen I fibrillogenesis and for normal cardiovascular development. Proc. Natl. Acad. Sci. U. S. A. 94, 1852–1856.

Liu, Y., Zhou, J., Zhao, W., Li, X., Jiang, R., Liu, C., et al., 2012. XBP1S associates with RUNX2 and regulates chondrocyte hypertrophy. J. Biol. Chem. 287, 34500–34513.

Liu, D.D., Zhang, J.C., Zhang, Q., Wang, S.X., Yang, M.S., 2013. TGF-β/BMP signaling pathway is involved in cerium-promoted osteogenic differentiation of mesenchymal stem cells. J. Cell. Biochem. 114, 1105–1114.

Maeda, T., Kawane, T., Horiuchi, N., 2003. Statins augment vascular endothelial growth factor expression in osteoblastic cells via inhibition of protein prenylation. Endocrinology 144, 681–692.

Maeda, T., Matsunuma, A., Kurahashi, I., Yanagawa, T., Yoshida, H., Horiuchi, N., 2004. Induction of osteoblast differentiation indices by statins in MC3T3-E1 cells. J. Cell. Biochem. 92, 458–471.

Maehata, Y., Takamizawa, S., Ozawa, S., Izukuri, K., Kato, Y., Sato, S., et al., 2007. Type III collagen is essential for growth acceleration of human osteoblastic cells by ascorbic acid 2-phosphate, a long-acting vitamin C derivative. Matrix Biol. 26, 371–381.

Min, K.S., Park, H.J., Lee, S.K., Park, S.H., Hong, C.U., Kim, H.W., et al., 2008. Effect of mineral trioxide aggregate on dentin bridge formation and expression of dentin sialoprotein and heme oxygenase-1 in human dental pulp. J. Endod. 34, 666–670.

Min, K.S., Yang, S.H., Kim, E.C., 2009. The combined effect of mineral trioxide aggregate and enamel matrix derivative on odontoblastic differentiation in human dental pulp cells. J. Endod. 35, 847–851.

Mizutani, A., Sugiyama, I., Kuno, E., Matsunaga, S., Tsukagoshi, N., 2001. Expression of matrix metalloproteinases during ascorbate-induced differentiation of osteoblastic MC3T3-E1 cells. J. Bone Miner. Res. 16, 2043–2049.

Mori, K., 2000. Tripartite management of unfolded proteins in the endoplasmic reticulum. Cell 101, 451–454.

Murakami, T., Saito, A., Hino, S., Kondo, S., Kanemoto, S., Chihara, K., et al., 2009. Signalling mediated by the endoplasmic reticulum stress transducer OASIS is involved in bone formation. Nat. Cell Biol. 11, 1205–1211.

Nakashima, K., Zhou, X., Kunkel, G., Zhang, Z., Deng, J.M., Behringer, R.R., et al., 2002. The novel zinc finger-containing transcription factor osterix is required for osteoblast differentiation and bone formation. Cell 108, 17–29.

Parirokh, M., Torabinejad, M., 2010. Mineral trioxide aggregate: a comprehensive literature review — part III: clinical applications, drawbacks, and mechanism of action. J. Endod. 36, 400–413.

Price, P.A., Baukol, S.A., 1980. 1,25-Dihydroxyvitamin D_3 increases synthesis of the vitamin K-dependent bone protein by osteosarcoma cells. J. Biol. Chem. 255, 11660–11663.

Qin, H., Cai, J., Fang, J., Xu, H., Gong, Y., 2010. Could MTA be a novel medicine on the recurrence therapy for GCTB? Med. Hypotheses 74, 368–369.

Roy, B., Li, W.W., Lee, A.S., 1996. Calcium-sensitive transcriptional activation of the proximal CCAAT regulatory element of the grp78/BiP promoter by the human nuclear factor CBF/NF-Y. J. Biol. Chem. 271, 28995–29002.

Saito, A., Ochiai, K., Kondo, S., Tsumagari, K., Murakami, T., Cavener, D.R., et al., 2011. Endoplasmic reticulum stress response mediated by the PERK-eIF2α-ATF4 pathway is involved in osteoblast differentiation induced by BMP2. J. Biol. Chem. 286, 4809–4818.

Tohmonda, T., Miyauchi, Y., Ghosh, R., Yoda, M., Uchikawa, S., Takito, J., et al., 2011. The IRE1α-XBP1 pathway is essential for osteoblast differentiation through promoting transcription of osterix. EMBO Rep. 12, 451–457.

Wang, X., Schroder, H.C., Feng, Q., Diehl-Seifert, B., Grebenjuk, V.A., Muller, W.E., 2014a. Isoquercitrin and polyphosphate co-enhance mineralization of human osteoblast-like SaOS-2 cells via separate activation of two RUNX2 cofactors AFT6 and Ets1. Biochem. Pharmacol. 89, 413–421.

Wang, Y., Li, J., Song, W., Yu, J., 2014b. Mineral trioxide aggregate upregulates odonto/osteogenic capacity of bone marrow stromal cells from craniofacial bones via JNK and ERK MAPK signalling pathways. Cell Prolif. 47, 241–248.

Wu, B.C., Huang, S.C., Ding, S.J., 2013. Comparative osteogenesis of radiopaque dicalcium silicate cement and white-colored mineral trioxide aggregate in a rabbit femur model. Materials 2013, 5675–5689.

Yazdizadeh, M., Bouzarjomehri, Z., Khalighinejad, N., Sadri, L., 2013. Evaluation of apical microleakage in open apex teeth using MTA apical plug in different sessions. ISRN Dent. 2013, 959813.

Ye, J., Rawson, R.B., Komuro, R., Chen, X., Dave, U.P., Prywes, R., et al., 2000. ER stress induces cleavage of membrane-bound ATF6 by the same proteases that process SREBPs. Mol. Cell 6, 1355–1364.

Yeung, Y.G., Stanley, E.R., 2009. A solution for stripping antibodies from polyvinylidene fluoride immunoblots for multiple reprobing. Anal. Biochem. 389, 89–91.

Zhang, C., Tang, W., Li, Y., 2012. Matrix metalloproteinase 13 (MMP13) is a direct target of osteoblast-specific transcription factor osterix (Osx) in osteoblasts. PLoS One 7, e50525.

Zhao, X., He, W., Song, Z., Tong, Z., Li, S., Ni, L., 2012. Mineral trioxide aggregate promotes odontoblastic differentiation via mitogen-activated protein kinase pathway in human dental pulp stem cells. Mol. Biol. Rep. 39, 215–220.